

**KERNFORSCHUNGSZENTRUM
KARLSRUHE**

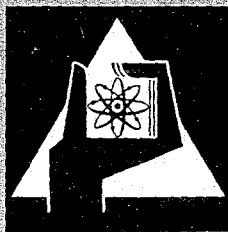
Dezember 1966

KFK 492

Institut für Neutronenphysik und Reaktortechnik

Experimental Local Heat-Transfer and Average Friction Coefficients for
Subsonic Turbulent Flow of Air in an Annulus at High Temperatures

M. Dalle Donne, E. Meerwald



GESELLSCHAFT FÜR KERNFORSCHUNG M. B. H.

KARLSRUHE



EXPERIMENTAL LOCAL HEAT-TRANSFER AND AVERAGE FRICTION COEFFICIENTS FOR SUBSONIC TURBULENT FLOW OF AIR IN AN ANNULUS AT HIGH TEMPERATURES*

M. DALLE DONNE† and E. MEERWALD‡

(Received 24 February 1966)

Abstract—Experimental local heat-transfer and friction coefficients are correlated for subsonic turbulent flow of air through a high temperature annulus (maximum wall temperature: 1000°C) with long unheated entrance length.

The recommended formulae are:

$$Nu_B = 0.0181 \left(\frac{D_2}{D_1} \right)^{0.2} Re_B^{0.8} Pr_B^{0.4} \left(\frac{T_w}{T_e} \right)^{-0.18}$$

$$f_B = 0.0615 \left(\frac{D_2/D_1 - 1}{D_2/D_1} \right)^{0.1} Re_w^{-0.22}$$

NOMENCLATURE

Geometrical parameters

- A , $(\pi/4)(D_2^2 - D_1^2)$ = cross-sectional area of the test section [cm²];
- D_1 , diameter of the inner cylinder of the annulus [cm];
- D_2 , diameter of the outer cylinder of the annulus [cm];
- D , annulus hydraulic diameter = $(4A/P)$ = $D_2 - D_1$ [cm];
- l , distance from the inlet of the section considered (the unheated entrance length not included) [cm];
- L , total length of heated test section [cm];

- P , $\pi(D_2 + D_1)$ = wetted perimeter of the test section cross section [cm];
- S_1 , $\pi D_1 L/10$ = outer surface of $\frac{1}{10}$ th of the inner tube [cm²];
- S_2 , $\pi D_2 L/10$ = inner surface of $\frac{1}{10}$ th of the outer tube [cm²].

Gas properties

- c_p , specific heat at constant pressure [cal/g degC];
- k , thermal conductivity [cal/cm s degC];
- R , gas constant [cm²/s² degK];
- γ , specific heat ratio [dimensionless];
- μ , dynamic viscosity [g/cm s];
- ρ , density [g/cm³].

Temperatures

- T_B , $T_T - (v_B^2/2 \cdot 10^7 J c_p)$ = absolute static bulk temperature of the gas [°K];
- T_E , absolute total gas temperature at the test section entrance \cong absolute static gas temperature at the entrance (because the gas velocity is very small there) [°K];

* This paper has been prepared within the framework of the association Euratom-Gesellschaft für Kernforschung mbH. in the field of fast breeder development.

† Delegated from Euratom to the Fast Breeder Project, Institute of Neutron Physics and Reactor Engineering, Kernforschungszentrum, Karlsruhe, West Germany.

‡ Gesellschaft für Kernforschung mbH., Institute of Neutron Physics and Reactor Engineering, Kernforschungszentrum, Karlsruhe, West Germany.

T_T ,	$T_E + (Q_g/Mc_p) =$ absolute total bulk temperature of the gas [$^{\circ}\text{K}$];		from inner tube to outer tube for $\frac{1}{10}$ th of test section [cal/s];
T_{W_i} ,	$T_{W_i} =$ absolute temperature of the wall of the inner tube [$^{\circ}\text{K}$];	q'_{g1} ,	$q_{gi}/(L/10) =$ heat given to gas directly by inner tube for unit test section length [cal/cm s];
T_{W_a} ,	$T_B + r(T_T - T_B) =$ absolute adiabatic wall temperature ($^{\circ}\text{K}$), where $r =$ recovery factor, for air, smooth tube section and turbulent flow, r is equal to 0.84 [7];	v_B ,	$M/A\rho_B = MRT_B/Ap =$ velocity of the bulk of the gas [cm/s];
T_{W_M} ,	maximum value for each run of the absolute wall temperature of the inner tube [$^{\circ}\text{K}$];	ϵ_{11} ,	total emissivity of the outer surface of inner tube [dimensionless];
T_{W_o} ,	absolute temperature of the wall of the outer tube [$^{\circ}\text{K}$];	ϵ_{21} ,	total emissivity of the inner surface of the outer tube [dimensionless];
T_{∞} ,	absolute static gas temperature at the outer edge of the thermal boundary layer for a free stream geometry [$^{\circ}\text{K}$].	ϵ_{12} ,	$\frac{1}{1/\epsilon_1 + S_1/S_2(1/\epsilon_2 - 1)}$ [dimensionless];
		σ ,	Stefan-Boltzmann constant [$\text{cal/cm}^2 \text{ s degK}^4$];
		τ_w ,	shear stress at the wall [dynes/cm^2].

Other physical parameters

h ,	convective heat-transfer coefficient between inner tube surface and gas bulk [$\text{cal/cm}^2 \text{ s degC}$];
G ,	$(M/A) =$ mass velocity of gas through test section [$\text{g/cm}^2 \text{ s}$];
J ,	conversion factor from heat units to work units = 4.187 W s/cal;
M ,	mass flow rate of gas [g/s];
p ,	absolute static pressure of the gas [dynes/cm^2];
Q_g ,	quantity of heat given to gas from entrance to the considered cross section of the annulus [cal/s];
q_e ,	heat produced by Joule effect in a segment equal to $\frac{1}{10}$ th in length of the inner tube [cal/s];
q_g ,	heat given to gas in $\frac{1}{10}$ th of the test section [cal/s];
q_{g1} ,	heat given to gas directly by the inner tube in $\frac{1}{10}$ th of the test section [cal/s];
q_{g2} ,	heat given to gas by the outer tube in $\frac{1}{10}$ th of the test section [cal/s];
q_1 ,	heat lost radially by conduction through insulation for $\frac{1}{10}$ th of test section [cal/s];
q_r ,	heat transmitted radially by radiation

Dimensionless groups

f_B ,	$2\tau_w/p_B v_B^2 =$ Fanning friction coefficient (or friction factor) evaluated at the gas bulk temperature T_B ;
Ma ,	$V_B/\sqrt{(\gamma p/\rho_B)} =$ mach number evaluated at the gas bulk temperature T_B ;
Nu_B ,	$hD/k_B =$ Nusselt number evaluated at the gas bulk temperature T_B ;
Pr_B ,	$\mu_B c_{pB}/k_B =$ Prandtl number evaluated at the gas bulk temperature T_B ;
Re_B ,	$\rho_B v_B D/\mu_B =$ Reynolds number evaluated at the gas bulk temperature T_B ;
Re_W ,	$\rho_W v_B D/\mu_W =$ Reynolds number evaluated at the wall temperature T_W .

Subscripts

B ,	gas properties evaluated at the gas bulk temperature T_B ;
W ,	gas properties evaluated at the wall temperature T_W .

1. INTRODUCTION

IN FAST reactor cores very high power densities are present. If gas or superheated steam cooling is used, the fuel element wall temperatures must be very high. During transients temperatures as high as 1000°C or above are likely. It is therefore of interest to investigate the effect of such high temperatures on heat-transfer

coefficient and friction factor for geometries similar to those adopted in fast reactor cores. The temperature effect is already well known for circular tube geometries [1], so it was decided to use in the experiment a geometry more similar to the one to be used in the core (bundle of parallel cylindrical rods), but still sufficiently simple to allow accuracy of results and simplification of experimental equipment. The annulus geometry with power production in the central rod is such a geometry.

It was felt that not sufficiently reliable data were available regarding temperature effects on annuli, thus an experiment was planned. The results of this experiment are reported in this paper. The future programme of this experiment includes the study of the effect of high temperatures on artificial roughness, which is also of great importance for gas or superheated steam cooled fast reactor cores, as well as experiments with smooth surfaces with vertical test sections rather than horizontal. With the vertical arrangement it should be possible to run at even higher wall temperatures without producing unduly high eccentricities between inner and outer tube.

Although the gases foreseen as possible reactor coolants are helium, CO_2 or water superheated steam, air is the coolant used in the present experiment. This simplifies the experiment very

much. In references [1] and [2] it has been shown that it is possible to obtain with air formulae valid for other gases as well, also for convective heat transfer in the presence of high temperature differences between wall and gas, provided the correlation formulae are chosen properly.

2. EXPERIMENTAL APPARATUS

A schematic diagram of the equipment used in the experiment is shown in Fig. 1.

A turboblower (maximum air flow 0.45 kg/s, pressure head 0.34 atm) driven by a 41-kW electrical motor delivers air successively through an orifice plate assembly to measure flow rate, an adiabatic entrance length, an annulus formed by a stainless-steel heater rod supported concentrically in a tube and finally to atmosphere.

Electrical supply for the test section is obtained from a fixed ratio transformer (20 V, 2000 A maximum), the primary winding of this transformer being supplied by a voltage regulator, the output voltage of which may be varied from 0 to 220 V. The voltage regulator is connected to the supply net through a voltage stabilizer. Thus the power supply can be continuously varied from 0 to 40 kW and any value in this range can be kept constant within ± 0.5 per cent.

The test section is shown in Fig. 2. The

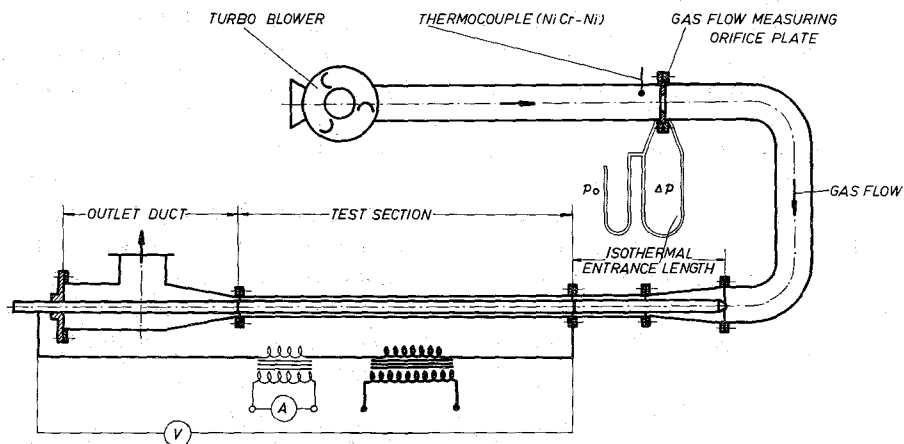


FIG. 1. General layout of rig.

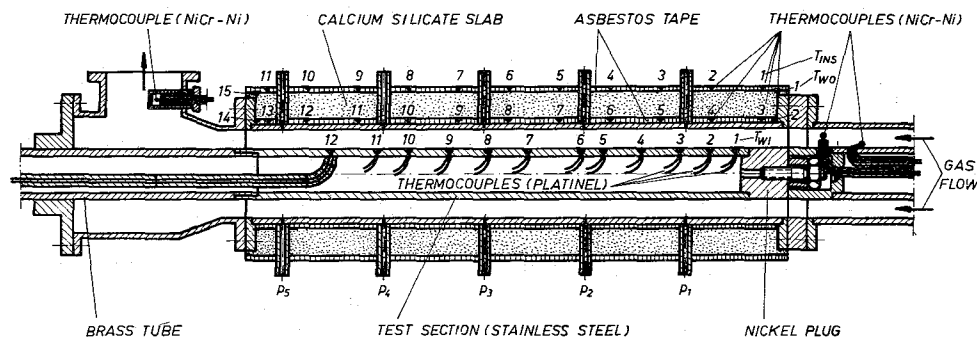


FIG. 2. Test section.

electrical current supplied to the test section is measured by means of a standard ammeter (end of scale 5 A) which is connected to a 400:1 ratio current transformer. To avoid errors caused by high resistance connecting cables, test section voltages are measured by means of a valve voltmeter.

The temperature of the internal tube heated surface is measured by means of 12 Platinel thermocouples introduced in the center of the heater element and electrically insulated with twin bore alumina tubing and then taken into the wall of the stainless steel tube where they are peened over. Subsequently the outer surface of the inner tube is made smooth again to avoid local turbulence. The Platinel thermocouples are high temperature resistant, but with a e.m.f. output four times higher than Platinum-Platinum-Rhodium (13 per cent) and considerably cheaper [3]. Thus they have been considered preferable.

The thermocouples are taken to two multiple trace Honeywell-Brown recorders to give an indication of temperature distribution and stability of conditions before taking a set of readings. One of the thermocouples is also connected to an automatic switch which switches off the heating power when the temperature measured by the thermocouple reaches a pre-set value. The temperature readings are performed by means of a Negretti and Zambra quick reading potentiometer (precision of the instru-

ment: $5 \mu\text{V}$, i.e. 0.1 degC). The voltage pick-up error in the thermocouples is negligible because the heating power is given by alternating current.

The outside tube of the annulus is insulated by a 50-mm thick calcium silicate slab contained between two layers of asbestos tape each about 7-mm thick. 15 CrNi-Ni thermocouples are welded to the outer surface of this tube and another 11 thermocouples are welded to little nickel plates placed between the calcium silicate slab and the asbestos outer layer. These thermocouples allow measurement of the temperature gradient in radial direction in the thermal insulation and therefore to measure the heat losses along the test section.

In five sections each 400-mm apart along the test section are placed static pressure measuring devices. In each section there are 4 pressure tappings at 90° . Thus one has the average static pressure in the section independently from local asymmetries. In practice the 4 measured values in any section differed very little.

Pressures are measured by means of U-tube manometers, either with water or mercury as manometric fluid. The gas temperature at the test section outlet is measured by means of a shielded Platinel thermocouple. No particular arrangement of gas mixing chamber is provided to reduce gas temperature measurement error, due to the very high gas velocities used. However, the Platinel thermocouple cannot see the heater

rod, thus avoiding errors due to direct radiation from a high temperature surface.

The gas temperature at the test section inlet is measured by means of a bare CrNi-Ni thermocouple in the gas stream. Another CrNi-Ni is soldered on the nearby wall of the adiabatic entrance length inner tube to check for possible errors due to heat conduction from the test section to the thermocouples. The temperature of this second thermoelement was never more than 1 degC above the one indicated by the first one, thus showing that the conduction error is negligible.

The gas temperature measurements are checked at every test by means of a comparison between the measured electrical power and the thermal power (heat to gas plus heat losses through insulation). Tests with heat balances more than 5 per cent out were rejected.

Gas flow is measured with an orifice plate with corner tappings installed according to British Standard 1042. Plates with orifices of various diameters are available for the measurement of the gas flow within a large range with a reasonable accuracy (probable error ± 1.5 per cent).

The distribution of the power produced by Joule effect in the heater rod is known by measuring the voltage distribution along the tube. One leg of each thermocouple fixed on the inner tube is used as a voltage tapping.

3. TEST SECTIONS AND RANGE OF OPERATING CONDITIONS

The test sections are 185.5-cm long. The stainless steel inner heater rod is connected at the outlet to a brass tube which, due to its very small resistivity, produces a negligible quantity of heat by Joule effect.

Experiments have been performed with two test sections:

- (a) diameter of the inner tube = $D_1 = 2.54$ cm;
 diameter of the outer tube = $D_2 = 5.38$ cm;

$$D_2/D_1 = 2.12;$$

$$\text{hydraulic diameter} = D = D_2 - D_1 = 2.84 \text{ cm};$$

$$L/D = 65.3.$$

(b) $D_1 = 5.08$ cm;

$$D_2 = 7.00 \text{ cm};$$

$$D_2/D_1 = 1.378;$$

$$D = 1.92 \text{ cm};$$

$$L/D = 96.6.$$

Experimental results have been obtained for the following range of conditions:

gas used: air;

gas inlet temperature: varied from 60°C to 80°C;

tube surface temperature: varied from 100°C to 1000°C;

Reynolds number (based on bulk temperature): varied from $2 \cdot 10^4$ to $1.8 \cdot 10^5$;

Mach number: up to 0.4;

T_w/T_B : up to 2.7;

T_w/T_E : up to 3.5.

4. STATIC CALIBRATION

As mentioned in Section 2 the heat losses are measured by thermocouples placed in the thermal insulation. However, this method is not very precise due to uncertainty in the values of the thermal conductivity of the insulation material. Thus for any insulation a calibration was performed. With the air supply turned off, the electrical current through the test section is adjusted to raise the temperature of the inner tube to a certain value. When steady temperature conditions are reached, measurements of voltage and temperature such as those shown in Fig. 3 are made. The temperatures on the wall of the inner and outer tubes are constant in the central portion of the test section for a considerable length. Over this section all the heat produced in the inner tube is lost radially outwards by radiation from the inner tube to the outer one and by conduction through the tube insulation. This heat may be calculated from the electrical input to the section. By repeating this experiment at

convenient temperature intervals until the temperature of the inner tube reaches 1000°C, it is possible to construct the graph of Fig. 3, which shows the heat losses through the thermal insulation for $\frac{1}{10}$ th of the length of the test section as function of the outer tube wall temperature.

The static calibration allows also the measurement of the relative total emissivity ε_{12} between the two concentric tubes as a function of temperature. For the central portion of the test section where the temperatures T_{Wi} and T_{Wo} are constant, one can assume with a good approximation that the heat moves by radiation only in radial direction. Thus one can use the formula valid for infinitely long concentric tubes:

$$q_r = \frac{\sigma S_1}{(1/\varepsilon_1) + (S_1/S_2)[(1/\varepsilon_2) - 1]} (T_{Wi}^4 - T_{Wo}^4) = \varepsilon_{12} \sigma S_1 (T_{Wi}^4 - T_{Wo}^4). \quad (1)$$

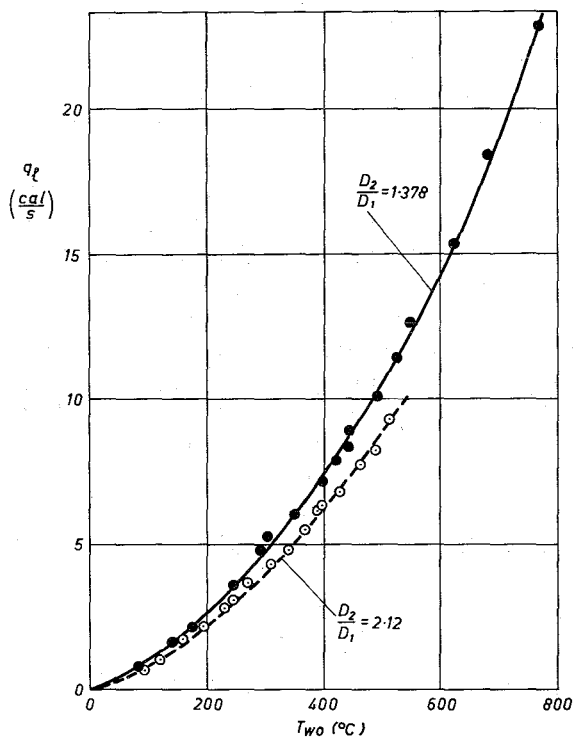


FIG. 3. Radial heat losses through the thermal insulation for $\frac{1}{10}$ th of the length of the test section.

The emissivity coefficient depends on both temperatures T_{Wi} and T_{Wo} , but in first approximation, $\varepsilon_{12} \cong \varepsilon_1$ because $S_1/S_2 < 1$ and we can assume that ε_{12} depends only on T_{Wi} . Figure 4 shows ε_{12} , obtained with the static calibrations using equation (1), as a function of T_{Wi} .

5. ANALYSIS OF DATA

5.1 Heat flux and temperature distribution

Figure 5 shows a typical example of temperature, pressure and voltage distribution along the test section. The temperatures of inner and outer tubes are directly measured with thermocouples. Voltage distribution along the inner tube and pressure distribution along the annulus are also measured values. One can see that at about 150 cm from the beginning of the test section the wall temperature of the inside and outside tubes has a sudden decrease. This is due to local turbulence due to a small ceramic support which keeps the inner tube concentric with the outer one. This effect is confined to a small region at the outlet of the test section where the conduction end effect is already strong. This portion of test section is not considered in the computation of the results.

The bulk gas total temperature, also shown, is calculated in the following way. The test section is divided in ten equal parts along the length. For each part the heat produced in the inner tube by Joule effect (q_e) is calculated knowing the electrical current and the voltage drop in that particular section. From the average value of T_{Wo} of the section and the graph of Fig. 3 one obtains the heat loss through the lagging (q_1). The difference between heat produced and heat lost gives the heat to the gas (q_g). Dividing this by the gas mass flow one obtains the increment in enthalpy of the gas in this section. The gas enthalpy at the inlet of the annulus is obtained from the gas temperature and pressure which are known. From the gas enthalpy and pressure distribution along the test section one can calculate the total gas bulk temperature along the annulus.

The gas physical properties are from [4]. To

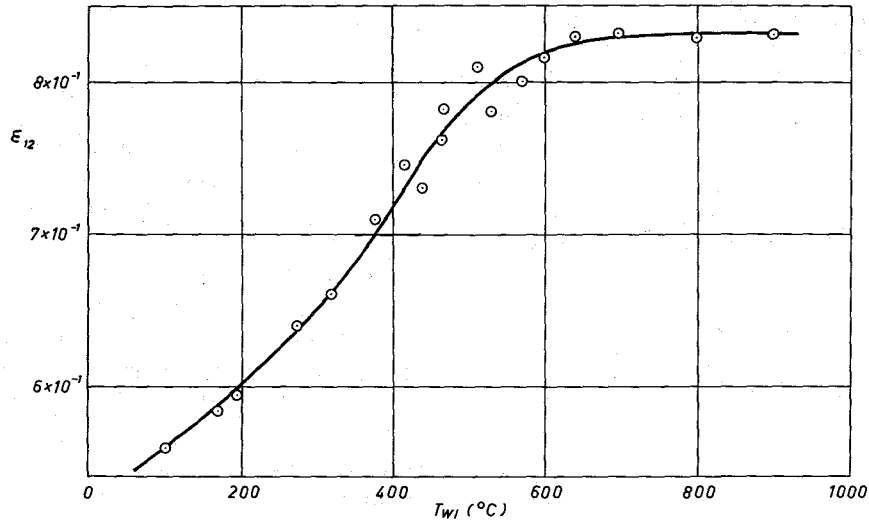


FIG. 4. Emissivity between the inner and outer tube as a function of the inner tube temperature. Obtained from static calibration.

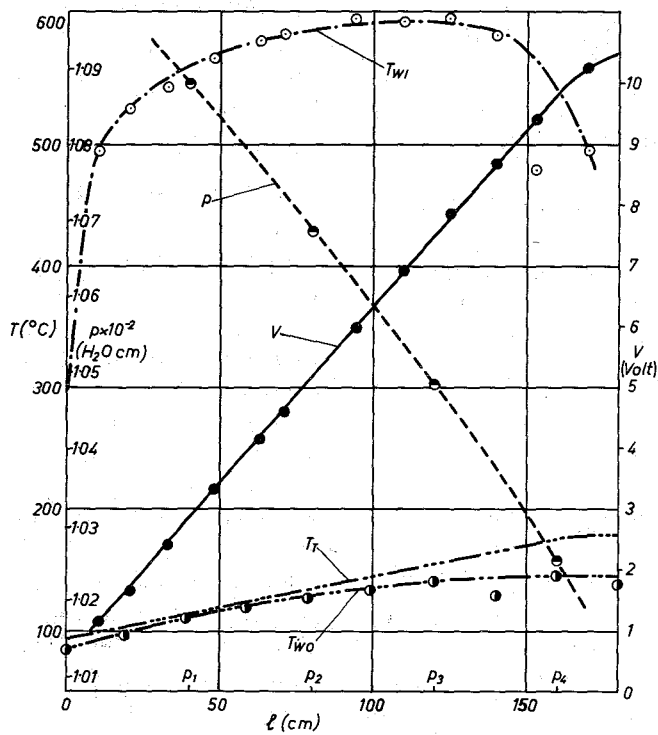


FIG. 5. Pressure, voltage, heater rod temperature (T_{W1}), outer tube (T_{W0}) and gas bulk total temperature (T_T) typical distribution along test section ($D_2/D_1 = 2.12$ test section, $Re_B = 1.05 \times 10^5$).

calculate the heat which goes by convection from the inner tube directly to the gas, it is necessary to subtract from q_g the heat which goes by radiation from the inner tube to the outer tube and then by convection from the outer tube to the gas (q_{g2}). q_{g2} is given by the difference between q_r , which one can obtain knowing T_{Wb} , T_{Wo} and ε_{12} from Fig. 4, and q_1 .

Thus:

$$\begin{aligned} q_{g1} &= q_g - q_{g2} = q_g - (q_r - q_1) \\ &= q_e - q_1 - q_r + q_1 = q_e - q_r \end{aligned} \quad (2)$$

In this one assumes that the gas is perfectly transparent to thermal radiation, which for air is a very good approximation.

5.2 Friction coefficients

The friction coefficients were calculated from the equation:

$$f_B = - \frac{D}{2p\gamma Ma^2} \frac{\partial}{\partial l} [p(1 + \gamma Ma^2)] \quad (3)$$

which requires the measurement of gas mass flow, pressure and total gas temperature along the test section. Equation (3) takes into account the pressure drop due to acceleration and it is obtained in Appendix 1. Using equation (3), it is not necessary to calculate directly the static gas bulk temperature T_B , although the fluid properties are evaluated at T_B , as they should, and not at T_T .

5.3 Heat-transfer coefficients

To avoid errors in calculation caused by end effects and heat conduction along the test section wall, attention was confined to local values in the center of the annulus. Calculations were performed for three cross sections 50, 90 and 130 cm distant from the point where the heating starts. This corresponds to distances of 17.6, 31.7 and 45.8 l/D for the test section $D_2/D_1 = 2.12$ and 26.05, 46.9 and 67.7 l/D for the test section $D_2/D_1 = 1.378$. The heat-transfer coefficient was calculated with

the equation:

$$h = \frac{q'_{g1}}{(T_W - T_T) \pi D_1} \quad (4)$$

The Nusselt number was calculated from $Nu_B = (hD/k_B)$, the Prandtl number from $Pr_B = \mu_B c_{pB}/k_B$ and the corresponding Reynolds number from $Re_B = MD/A\mu_B$.

The air properties are from reference [4]. They were evaluated at the total gas bulk temperature T_T , directly obtained by the gas measurement at the inlet of the test section plus the heat to the gas (see paragraph 5.1), instead of the static gas bulk temperature T_B . However, the Mach number being relatively small, the difference between the two temperatures is never above 20 degC, and the error in $Nu_B/Re_B^{0.8} Pr_B^{0.4}$ is always below 1.5 per cent. On the other hand one should use T_{Wa} in place of T_T in equation (4). This produces in the worst case an error of 3 degC, that is 1 per cent in Nu_B in the opposite direction of the previous. The resulting maximum possible error of 0.5 per cent is well within the accuracy of the measurement.

6. LOCAL HEAT-TRANSFER COEFFICIENTS

6.1 Correlation with T_W/T_B

Figures 6 and 7 show the ratio $Nu_B/Re_B^{0.8} Pr_B^{0.4}$ versus T_W/T_B for various l/D 's and two different values of D_2/D_1 . In this, one assumes that the Reynolds number effect is at the exponent 0.8, how it was found by almost all the previous authors for fluids in turbulent regime, and the Prandtl number effect is at the exponent 0.4. The exponent of Pr_B is usually taken as 0.4 although in some cases other values are given. Due to the very small variations of the Prandtl number for gases the precision with which it is possible to measure this exponent is very low. Conversely its variations have little effect on heat-transfer coefficients, e.g. the often used value 0.33 makes only 2.5 per cent difference on Nu_B .

As many authors before, we used the ratio T_B/T_W to take into account the effect of the

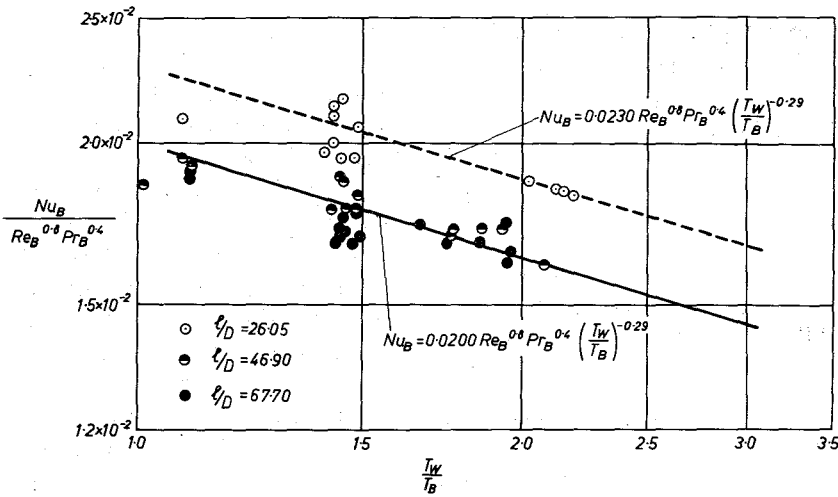


FIG. 6. $D_2/D_1 = 1.378$ test section. Heat-transfer results correlated at the bulk temperature versus T_W/T_B .

variations of fluid properties in any section of the annulus due to large temperature differences between wall and gas temperatures.

From the figures one can see that between the sections at 50 cm from the inlet and the subsequent ones there is still a considerable

l/D effect, which disappears for the sections 90 and 130 cm distant from the inlet. Thus one can say that, to achieve a fully established temperature profile, the flow requires 31.7 l/D in the case $D_2/D_1 = 2.12$ and 46.9 l/D in the case $D_2/D_1 = 1.378$.

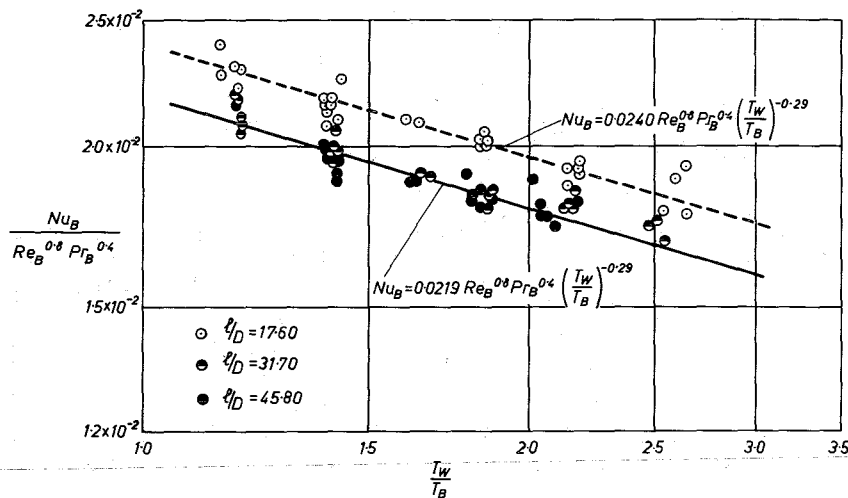


FIG. 7. $D_2/D_1 = 2.12$ test section. Heat-transfer results correlated at the bulk temperature versus T_W/T_B .

The equations which correlate the points in fully established flow are the following:

$$Nu_B = 0.0200 Re_B^{0.8} Pr_B^{0.4} \left(\frac{T_W}{T_B}\right)^{-0.29}$$

for $\frac{D_2}{D_1} = 1.378$ (5)

and

$$Nu_B = 0.0219 Re_B^{0.8} Pr_B^{0.4} \left(\frac{T_W}{T_B}\right)^{-0.29}$$

for $\frac{D_2}{D_1} = 2.12$. (6)

Equations (5) and (6) can be correlated by the equation:

$$Nu_B = 0.0188 \left(\frac{D_2}{D_1}\right)^{0.2} Re_B^{0.8} Pr_B^{0.4} \left(\frac{T_W}{T_B}\right)^{-0.29}$$

(7)

6.2 Correlation with T_W/T_E

In recent time the ratio T_W/T_E has been used in place of T_W/T_B to correlate high temperature heat-transfer coefficients with forced convection of gases in tubes [1, 2, 5]. In these references a theory is outlined for understanding the reason of T_W/T_E instead of T_W/T_B , here a short explana-

tion is sufficient. The choice of the parameter T_W/T_E is suggested by the comparison of the growth of the thermal boundary layer in a duct (closed geometry) and along a flat plate (free-stream geometry). Only for a free-stream geometry is it possible to apply rigorously the Buckingham theory of dimensional analysis to the differential equations, Navier-Stokes' and Fourier's, and their boundary conditions, which govern the convective heat transfer. The temperature-dependent fluid properties are accounted by the ratio T_W/T_∞ . Because for a closed geometry T_E corresponds to T_∞ for a free stream geometry, the assumption of T_W/T_E as the characteristic temperature parameter implies that the thermal boundary layer in a duct develops, at least in the region nearest to the wall which is the most important for the heat-transfer coefficient, like that of a flat-plate. This assumption is perfectly reasonable because the thickness of the boundary laminar sublayer is always much smaller than the hydraulic radius of the duct.

Figures 8 and 9 show the ratio $Nu_B/Re_B^{0.8} Pr_B^{0.4}$ versus T_W/T_E for various l/D 's and two different values of D_2/D_1 . The scatter of these points is considerably less than that with T_W/T_B , especially for the test section $D_2/D_1 =$

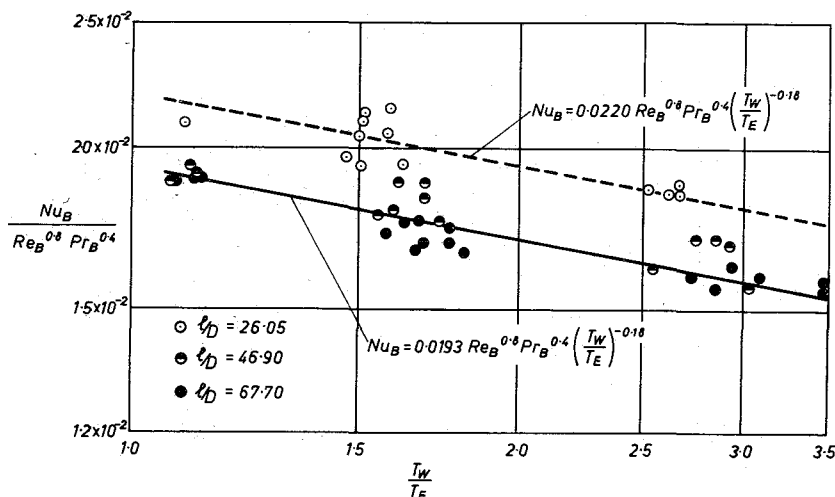


FIG. 8. $D_2/D_1 = 1.378$ test section. Heat-transfer results correlated at the bulk temperature versus T_W/T_E .

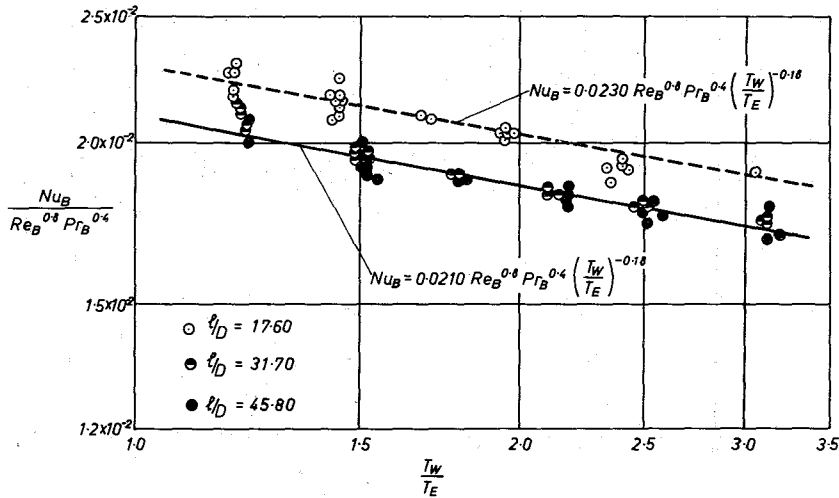


FIG. 9. $D_2/D_1 = 2.12$ test section. Heat-transfer results correlated at the bulk temperature versus T_w/T_E .

2.12 which gives better experimental results than the other. The l/D effect is slightly reduced.

The equations which correlate the points in fully established flow are the following:

$$Nu_B = 0.0193 Re_B^{0.8} Pr_B^{0.4} \left(\frac{T_w}{T_E}\right)^{-0.18}$$

for $\frac{D_2}{D_1} = 1.378$ (8)

and

$$Nu_B = 0.0210 Re_B^{0.8} Pr_B^{0.4} \left(\frac{T_w}{T_E}\right)^{-0.18}$$

for $\frac{D_2}{D_1} = 2.12$. (9)

Equations (8) and (9) can be correlated by the equation:

$$Nu_B = 0.0181 \left(\frac{D_2}{D_1}\right)^{0.2} Re_B^{0.8} Pr_B^{0.4} \left(\frac{T_w}{T_E}\right)^{-0.18} \quad (10)$$

6.3 The l/D effect

The l/D effect is quite evident from Figs. 6-9. To illustrate this effect more clearly the ratios

$$(Nu/Re_B^{0.8} Pr_B^{0.4})(T_w/T_B)^{0.29}$$

and

$$(Nu_B/Re_B^{0.8} Pr_B^{0.4})(T_w/T_E)^{0.18}$$

have been plotted respectively in Fig. 10 and 11 versus l/D for the two D_2/D_1 's and two values of Re_B . One can see that with the second type of correlation the l/D effect tends to disappear for values above $l/D \approx 25$ for $D_2/D_1 = 2.12$ and $l/D \approx 50$ for $D_2/D_1 = 1.378$, while in the T_w/T_B correlation the thermal entrance region seems to be slightly longer and the Reynolds effect not completely taken into account by the factor $Re_B^{0.8}$.

7. AVERAGED FRICTION COEFFICIENTS

7.1 Isothermal friction coefficients

Before starting the runs with heat transfer, some runs at room temperature, i.e. without heat production were carried out with both test sections. They are called generally isothermal runs, although adiabatic would be a better denomination.

The friction factors relative to the central portion of the annulus were calculated. They are shown in Figs. 12 and 13. For comparison the Blasius equation, valid for circular tubes, and the Davis equation [6], obtained by correlating various experimental data for annuli, are also shown in the figures.

The points of the present experiment are

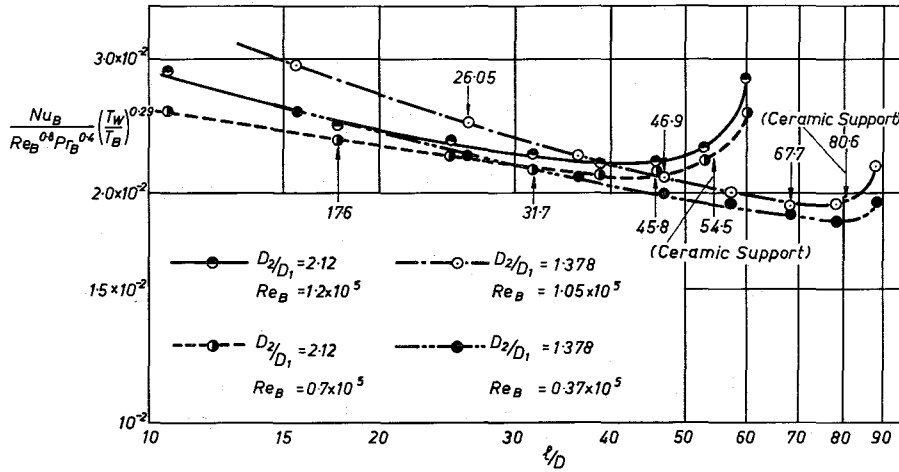


FIG. 10. Variation of Nusselt number, corrected for Re_B, Pr_B and T_W/T_B effect, with $1/D$.

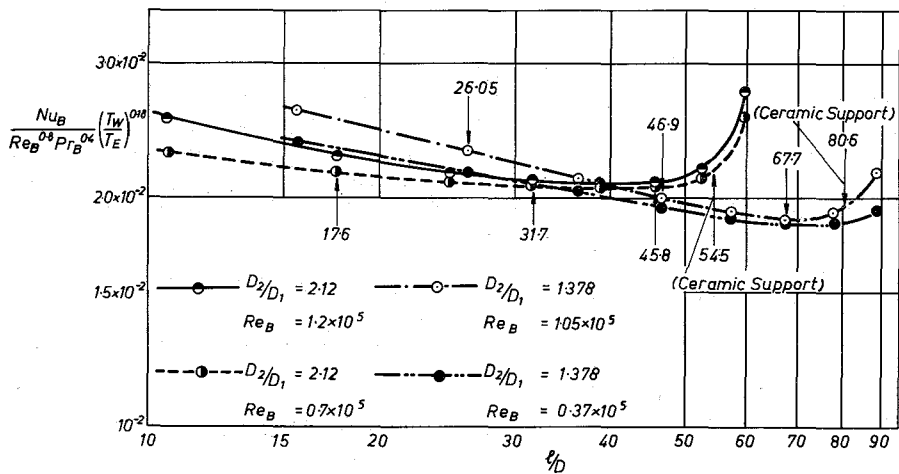


FIG. 11. Variation of Nusselt number, corrected for Re_B, Pr_B and T_W/T_E effect, with $1/D$.

correlated by the equations:

$$f_B = 0.0542 Re_B^{-0.22} \quad \text{for } \frac{D_2}{D_1} = 1.278 \quad (11)$$

and

$$f_B = 0.0573 Re_B^{-0.22} \quad \text{for } \frac{D_2}{D_1} = 2.12. \quad (12)$$

Equations (11) and (12) can be correlated by equation:

$$f_B = 0.0615 \left(\frac{D_2/D_1 - 1}{D_2/D_1} \right)^{0.1} Re_B^{-0.22}. \quad (13)$$

It is interesting to notice that the factor which takes into account the D_2/D_1 effect is the same as that suggested by Davis. The friction factors, however, are about 10 per cent lower than those of Davis in the Reynolds number range considered. The agreement with the Blasius correlation is better.

7.2 Friction coefficients with heat transfer

These were measured only with the $D_2/D_1 = 1.378$ test section. With the $D_2/D_1 = 2.12$ test

section only two pressure tappings were available, sufficient to obtain isothermal values, because in this case the pressure drops are linear in the central portion of the annulus, but not enough when the pressure profile along the test section is not linear due to fluid properties variations and acceleration losses.

With the $D_2/D_1 = 1.378$ test section, it was

possible to measure the static pressure in 5 different sections of the annulus. Local friction factors were calculated for the same sections where the heat-transfer coefficients were calculated ($l/D = 26.05, 46.9, 67.7$). It was found, however, that the scattering of the points was extremely high (± 31 per cent). This is due in part to the fact that they depend on the

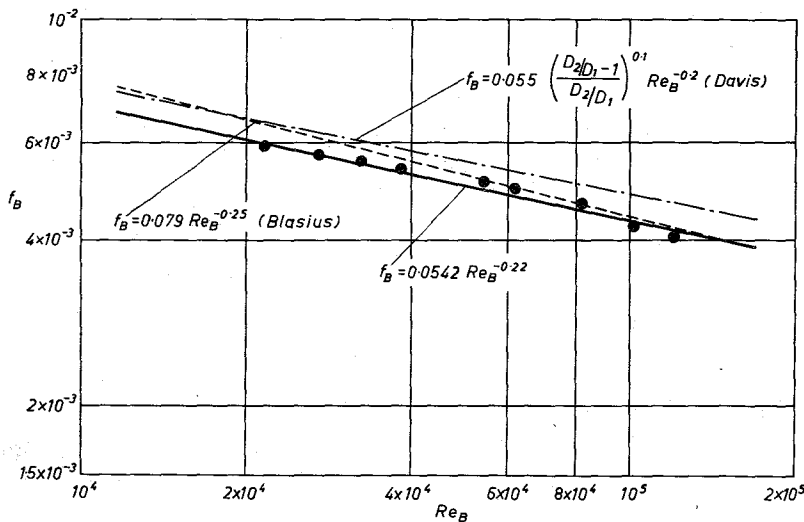


FIG. 12. Isothermal friction factor for $D_2/D_1 = 1.378$ annulus. Comparison with other authors.

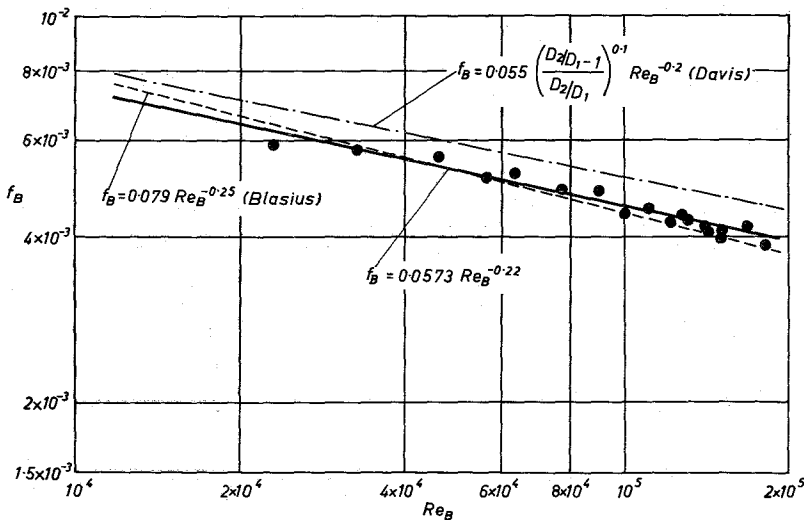


FIG. 13. Isothermal friction factor for $D_2/D_1 = 2.12$ annulus. Comparison with other authors.

difference of two pressures whose values are very close to each other [see equation (3)]. To reduce this error, it was decided to average the three local friction factors for each run. This means that a much bigger pressure difference along the test section is considered and the pressure difference measurement percentage error should be less. Figure 14 shows such averaged friction coefficients, times

$$Re_B^{0.22} [(D_2/D_1 - 1)/D_2/D_1]^{-0.1}$$

to take into account of the Reynolds and geometry effects obtained with the isothermal runs, versus T_W/T_E . The points can be correlated by the equation:

$$f_B = 0.0615 \left(\frac{D_2/D_1 - 1}{D_2/D_1} \right)^{0.1} \times Re_B^{-0.22} \left(\frac{T_W}{T_E} \right)^{0.25} \quad (14)$$

The scatter of the points is still quite high (± 20 per cent) and the correlation does not appear very satisfactory.

Dalle Donne and Bowditch [1] suggested that it was necessary to calculate the friction factor at the bulk temperature and the Reynolds number at the wall temperature to correlate their experimental results for gas flow in tubes

at high temperatures without any T_W/T_E or T_W/T_B factor. This method can be explained by a qualitative reasoning. Friction coefficients depend upon a balance of forces parallel to the axis of the tube, i.e. pressure drops, which are related to the total cross section area and therefore must be evaluated at the gas bulk temperature, and shear stresses which must be evaluated at the wall temperature, where they are originated.

Figure 15 shows the friction coefficients obtained with the $D_2/D_1 = 1.378$ test section with and without heat transfer plotted in the diagram f_B versus Re_W . All the points with the exception of four can be correlated within ± 10 per cent by the equation:

$$f_B = 0.0542 Re_W^{-0.22} \quad (15)$$

Thus, if one assumes that the geometry effect is the same with and without heat transfer, the recommended formula is:

$$f_B = 0.0615 \left(\frac{D_2/D_1 - 1}{D_2/D_1} \right)^{0.1} Re_W^{-0.22} \quad (16)$$

8. CONCLUSIONS

Local heat-transfer and averaged friction coefficients were measured for subsonic turbulent flow of air through an annulus with

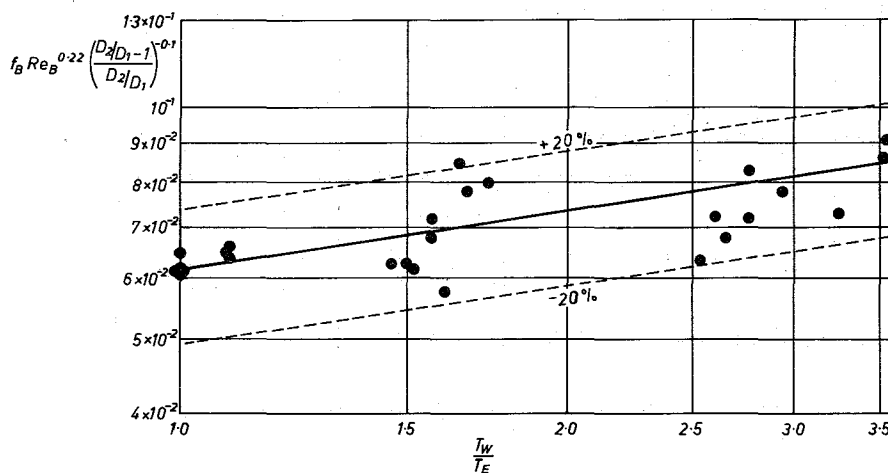


FIG. 14. Averaged friction coefficients versus T_W/T_E , $D_2/D_1 = 1.378$.

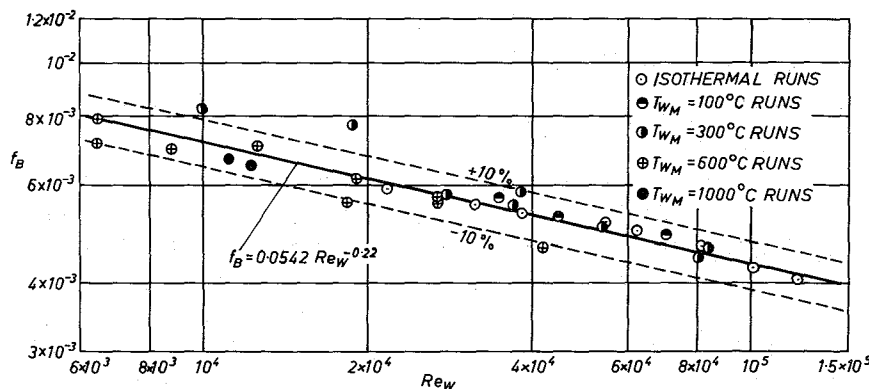


FIG. 15. $D_2/D_1 = 1.378$ test section. Friction coefficients correlated with Re_W , averaged in the central portion of the test section.

long unheated entrance length at wall temperatures up to 1000°C.

The local heat-transfer coefficients are correlated by:

$$Nu_B = 0.0181 \left(\frac{D_2}{D_1}\right)^{0.2} Re_B^{0.8} Pr_B^{0.4} \left(\frac{T_W}{T_E}\right)^{-0.18}$$

The friction coefficients averaged in the central portion of the annulus are correlated by:

$$f_B = 0.0615 \left(\frac{D_2/D_1 - 1}{D_2/D_1}\right)^{0.1} Re_W^{-0.22}$$

ACKNOWLEDGEMENTS

The authors wish to thank Mr. D. Artz and Mr. K. Kaldewey for their help in the construction of the rig, in performing the measurements, the numerical calculations and the graphs.

REFERENCES

1. M. DALLE DONNE and F. H. BOWDITCH, Experimental local heat transfer and friction coefficients for subsonic laminar, transitional and turbulent flow of air or helium in a tube at high temperatures, Dragon Project Report 184, April 1963.
2. M. DALLE DONNE and F. H. BOWDITCH, Local heat transfer and average friction coefficients for subsonic laminar, transitional and turbulent flow of air in a tube at high temperature, Dragon Project Report 88, March 1962.
3. M. DALLE DONNE, Tests and data concerning Platinel. A new high temperature thermocouple, Engelhard Industries Technical Bulletin, V (1), 5-9 (1964).
4. T. HILSEN RATH and Y. S. TOULOUKIAN, *Tables of thermodynamic and transport properties of Air, Argon, etc.* Pergamon Press, Oxford (1960).

5. M. DALLE DONNE, High temperature gas heat transfer in tubes, *Trans. ANS* 2 (2), 506 (1964).
6. E. S. DAVIS, *Trans. Am. Soc. Mech. Engrs* 65, 755 (1943).

APPENDIX I

Consider the flow of gas through a section of annulus of length dl and cross sectional area A , the equation of motion may be written:

force acting on gas in element $A dl$ - drag on surface = change in momentum over length dl or

$$A p - A(p + dp) - \tau_w \pi(D_1 + D_2) dl = M[(v_B + dv_B) - v_B]$$

therefore

$$\tau_w = - \frac{A dp + M dv_B}{\pi(D_1 + D_2) dl}$$

By definition:

$$\tau_w = f_B \frac{\rho_B v_B^2}{2}$$

Taking into account that in a duct $M = A \rho_B v_B$ is a constant and that $A = (\pi/4)(D_2^2 - D_1^2)$, one obtains:

$$f_B = - \frac{D_2 - D_1}{2 \rho_B v_B^2} \frac{\partial(p + \rho_B v_B^2)}{\partial l}$$

By definition

$$Ma = \frac{v_B}{\sqrt{(\gamma p / \rho_B)}}$$

thus

$$\rho_B v_B^2 = \gamma p Ma^2$$

and

$$f_B = -\frac{D}{2p\gamma Ma^2} \frac{\partial(p + \gamma p Ma^2)}{\partial l}$$

But

$$G = \frac{M}{A} = \rho_B v_B = \rho_B Ma \sqrt{\left(\frac{\gamma p}{\rho_B}\right)} = Ma \sqrt{(\gamma p \rho_B)}$$

$$\rho_B = \frac{p}{RT_B}$$

therefore

$$\rho_B = \frac{p}{R} \frac{[1 + (\gamma - 1/2) Ma^2]}{T_T}$$

therefore

$$G = Ma \sqrt{\left(\gamma p \frac{p}{R} \frac{[1 + (\gamma - 1/2) Ma^2]}{T_T}\right)}$$

or

$$\frac{G \sqrt{(RT_T)}}{p} = (\sqrt{\gamma}) Ma \left(1 + \frac{\gamma - 1}{2} Ma^2\right)^{\frac{1}{2}}$$

Hence using the relationship given in this last equation it is possible for various fixed values of γ to plot a family of curves

$$(\sqrt{\gamma}) Ma \left(1 + \frac{\gamma - 1}{2} Ma^2\right)^{\frac{1}{2}},$$

and therefore $G \sqrt{(RT_T)}/p$, versus Ma . Local values of G , T_T and p are directly measured, therefore the local values of Ma can be found quickly. It is possible to take into account the slight variation of γ with temperature by choosing the appropriate curve $G \sqrt{(RT_T)}/p$ versus Ma .

Résumé—Les coefficients expérimentaux de transport de chaleur et de frottement sont corrélés pour un écoulement subsonique turbulent d'air à travers une conduite annulaire portée à haute température (température pariétale maximale = 1000°C) avec une longue zone d'entrée non chauffée. Les formules recommandées sont:

$$Nu_B = 0,0181 \left(\frac{D_2}{D_1}\right)^{0,2} Re_B^{0,8} Pr_B^{0,4} \left(\frac{T_W}{T_E}\right)^{-0,18}$$

$$f_B = 0,0615 \left(\frac{D_2/D_1 - 1}{D_2/D_1}\right)^{0,1} Re_W^{-0,22}$$

Zusammenfassung—Für turbulente Unterschallströmung von Luft durch einen Ringspalt hoher Temperatur (maximale Wandtemperatur 1000°C) mit langer unbeheizter Anlaufstrecke sind die experimentell ermittelten Wärmeübergangs- und Reibungskoeffizienten korreliert. Die empfohlenen Gleichungen sind:

$$Nu_B = 0,0181 \left(\frac{D_2}{D_1}\right)^{0,2} Re_B^{0,8} Pr_B^{0,4} \left(\frac{T_W}{T_E}\right)^{-0,18}$$

$$f_B = 0,0615 \left(\frac{D_2/D_1 - 1}{D_2/D_1}\right)^{0,1} Re_W^{-0,22}$$

Аннотация—Определяются локальная теплопередача и потеря давления турбулентного потока в дозвуковой области при высоких температурах (максимальная температура стены: 1000°C) с большой необогреваемой длиной входа в кольцевой щели.

Обработка результатов опытов дала соотношения:

$$Nu_B = 0,0181 \left(\frac{D_2}{D_1}\right)^{0,2} Re_B^{0,8} Pr_B^{0,4} \left(\frac{T_W}{T_E}\right)^{-0,18}$$

$$f_B = 0,0615 \left(\frac{D_2/D_1 - 1}{D_2/D_1}\right)^{0,1} Re_W^{-0,22}$$